



Cai, L., Xu, W., and Luo, X. (2017) A double-distribution-function lattice Boltzmann method for bed-load sediment transport. *International Journal of Applied Mechanics*, 9(1), 1750013. (doi:[10.1142/S1758825117500132](https://doi.org/10.1142/S1758825117500132))

This is the author's final accepted version.

There may be differences between this version and the published version. You are advised to consult the publisher's version if you wish to cite from it.

<http://eprints.gla.ac.uk/137539/>

Deposited on: 06 April 2017

Enlighten – Research publications by members of the University of Glasgow  
<http://eprints.gla.ac.uk33640>

International Journal of Applied Mechanics  
© Imperial College Press

## A DOUBLE-DISTRIBUTION-FUNCTION LATTICE BOLTZMANN METHOD FOR BED-LOAD SEDIMENT TRANSPORT

LI CAI

*NPU-UoG International Cooperative Lab for Computation & Application  
in Cardiology, Northwestern Polytechnical University, Xian, 710129, China  
caili@nwpu.edu.cn*

WENJING XU\*

*NPU-UoG International Cooperative Lab for Computation & Application  
in Cardiology, Northwestern Polytechnical University, Xian, 710129, China  
xuwenjing9121@163.com*

XIAOYU LUO

*School of Mathematics and Statistics,  
University of Glasgow, Glasgow, G128QW, UK  
xiaoyu.luo@glasgow.ac.uk*

Received date

Accepted date

The governing equations of bed-load sediment transport are the shallow water equations and the Exner equation. To embody the advantages of the lattice Boltzmann method (e.g. simplicity, efficiency), the three-velocity (D1Q3) and five-velocity (D1Q5) double-distribution-function lattice Boltzmann models (DDF-LBMs), which can present the numerical solution for one-dimensional bed-load sediment transport, are proposed here based on the quasi-steady approach. The so-called DDF-LBM means we use two distribution functions to describe the movement of the two components, respectively. By using the Chapman-Enskog expansion, the governing equations can be recovered correctly from the DDF-LBMs. To illustrate the efficiency of these, two benchmark tests are used, and excellent agreements between the numerical and analytical solutions are demonstrated. In addition, we show that the D1Q5 DDF-LBM has better accuracy compared to the Hudson's method.

*Keywords:* Double-distribution-function; lattice Boltzmann method; bed-load sediment transport.

### 1. Introduction

In recent years, the research on fluvial dynamics in river channels has become a hot issue. There are many rivers in nature, which not only bring convenience to daily life but also disasters. For instance, the scour of river banks, the formation of the

\*Corresponding author.

turbidity, spreading of pollutants, all of these are important for the environment and business [Hudson and Sweby, 2003].

One of the main problems is sediment transport, which is caused by the interaction between the river and bed. Water flow induces sediment transport and changes the bed configuration, which in turn modify the flow structure. There are two sets of dynamics in the process, one is the flowing fluid described in the shallow water equations, and the other is sediment described in the bed-updating equation. They are coupled via the changing riverbed. When the flux is a function defined of  $u$  only, two approaches discussed by Cunge *et al.* can be used for the sediment transport [Cunge *et al.*, 1980]. The conventional method for this system is decoupling (quasi-steady) approach, which is based on the fundamental that the update speed of the riverbed is considerably smaller in magnitude than the water flow [Hudson, 2001]. In this quasi-steady process, the water flow is assumed to be steady, and the effects of river bed changing are ignored. That is, the system is decoupled into the hydrodynamic and the morphodynamic systems. It requires us to solve the shallow water equations in a fixed bed, and then followed by a bed-update. For the unsteady approach, the wave speed of the bed-updating equation is considered to be a similar magnitude to the wave speed of the water flow. Hence the system is discretised simultaneously.

With the emergence of the commercial finite difference codes, the decoupling approach has reached a climax [De Vriend *et al.*, 1993]. Many traditional methods, such as the finite difference method and finite volume method have been widely used to obtain the numerical solution for the system. However, there are problems in the calculating process [Liu *et al.*, 2014], such as the approximation of the wave speed for the bed-updating equation, the spurious oscillations, the advection and source terms approximation and so on, all of those factors affect the sediment transport's development.

Fortunately, the lattice Boltzmann method (LBM) can overcome some difficulties for simulating sediment transport with the lattice model. It is a mesoscopic numerical technique based on statistical physics, which simulates the fluid movement at the microscopic particle level. The method has been used in many different fields as a novel numerical method for computational fluid dynamics [Chen and Doolen, 1998; Moeendarbary *et al.*, 2009; Bég *et al.*, 2013; Aminfar *et al.*, 2015]. At the end of the 20th century, because of the unique features in the LBM, such as parallel computation, algorithmic simplicity, some researchers proposed extended theories of the LBM for non-linear partial differential equations and applied to river engineering. In 1999, Salmon used the LBM to study ocean circulation modeling [Salmon, 1999]. In 2002, Zhou developed a lattice Boltzmann model for shallow water equations with a source term [Zhou, 2002]. In 2009, Zhou proposed the LBM for solute transport [Zhou, 2009]. In 2010, Thang studied the lattice Boltzmann shallow equation and its coupling to build a canal network [Thang *et al.*, 2010]. In 2015, a new lattice Boltzmann approach for solving the 1D Saint-Venant equations

was developed [Liu *et al.*, 2015].

It is known that the sediment transport is caused by the interaction between river and bed. Clearly, two components, water flow and sediment, are in the system. According to the LBM theory, two kinds of the method can be used to solve this problem. One is the hybrid method, combining the LBM with traditional numerical methods, while the other is DDF-LBM, which uses two distribution functions to describe the movement of the two components respectively. To provide a competitive method for simulating sediment transport, two DDF-LBMs based on the quasi-steady approach are developed in this paper for the 1D bed-load sediment transport system constituting two hydrodynamic and one sediment equations. The D1Q3 DDF-LBM is the model whose flow distribution function and sediment distribution function are based on the three-velocity lattice. The D1Q5 DDF-LBM is the model whose flow distribution function is based on three-velocity lattice while sediment distribution function is based on the five-velocity lattice. Both DDF-LBMs fully embody the advantages of LBM. The efficiency and accuracy of these have been demonstrated by solving two benchmark tests.

## 2. DDF-LBM

In this section, the governing equations for 1D sediment transport are introduced firstly. Then the quasi-steady approach is analyzed with the characteristics of the system. Next, the D1Q3 and D1Q5 DDF-LBMs are described. And the recovery of the governing equations will be shown in detail.

### 2.1. Governing equations

According to the theory of sediment transport, when the sediment concentration is low, a 1D model can be described by the shallow water equations and Exner equation. Similar equations have been presented by Cunge *et al.* [Cunge *et al.*, 1980]. The shallow water equations, as classic fluid dynamic equations, are the section-averaged form of the Navier-Stokes equations, which represent the mass conservation and momentum conservation. The Exner equation accounts for the changes in the bed elevation or the conservation of sediment mass. So, in one-dimensional space, the complete system equations are

$$\frac{\partial h}{\partial t} + \frac{\partial hu}{\partial x} = 0, \quad (1)$$

$$\frac{\partial hu}{\partial t} + \frac{\partial}{\partial x} \left( hu^2 + \frac{1}{2}gh^2 \right) = -gh \frac{\partial B}{\partial x}, \quad (2)$$

$$\frac{\partial B}{\partial t} + \xi \frac{\partial q}{\partial x} = 0, \quad (3)$$

where  $t$  is time,  $x$  is the horizontal coordinates,  $h(x, t)$  is the flow depth above the bottom of the channel,  $u(x, t)$  is the depth-averaged velocity in the  $x$ -direction,  $g$  is

the gravitational acceleration,  $B(x, t)$  is the bed elevation, and  $q(u, h)$  is the total volumetric sediment transport rate in the  $x$ -direction. Here  $\xi = \frac{1}{1-\varepsilon}$ , and  $\varepsilon$  is the porosity of the bed, set to be 0.4 [Hudson and Sweby, 2003].

In order to solve the system of equations, the sediment transport formulate  $q$  must be known. There are many different forms of it and at different levels of complexity [Soulsby, 1997]. However, the most basic one is the sediment transport flux of Grass, which is used in this paper [Grass, 1981],

$$q(u) = Au |u|^{m-1}, \quad (4)$$

where  $A$  is a dimensional constant that encompasses the effects of grain size and kinematic viscosity with  $m$  being a constant between 1 and 4. And in order to ensure the sediment transport flux is valid for all values of  $u$ , we take  $m = 3$  [Hudson, 2001] giving

$$q(u) = Au^3. \quad (5)$$

## 2.2. Quasi-steady approach

In the most physical cases, the bed moves slower than the water flow, which justifies a quasi-steady approach. In the quasi-steady approach we assume that the water motions are steady with respect to changes in the bed level [Cunge *et al.*, 1980]. This allows us to discretize the water flow separately from the bed. Hence, we can use two distribution functions to simulate the movements of two components; one is for the shallow water equations, and the other is for the Exner equation. The detailed updating structure in the DDF-LBM is shown in Fig.1.

## 2.3. Lattice Boltzmann model for the shallow water equations

According to the quasi-steady approach, the water flow should be iterated to an equilibrium state before the bed updating. In this subsection, the D1Q3 flow lattice model will be used to solve the shallow water equations [Liu *et al.*, 2015]. In the LBM, the dynamics of it consists two steps: a streaming step, in which the particles move to neighbouring lattice points, and a collision step, where all lattices reach a new distribution equilibrium status [He *et al.*, 2008]. If the D1Q3 model is adopted, the corresponding lattice Boltzmann equation with the Bhatnagar-Gross-Krook (BGK) approximation for the shallow water equations is

$$f_\alpha(x + e_\alpha \Delta t, t + \Delta t) - f_\alpha(x, t) = -\frac{1}{\tau}(f_\alpha - f_\alpha^{eq}) + \frac{\Delta t}{N_\alpha e^2} e_\alpha F, \quad (6)$$

in which  $f_\alpha$  represents the distribution function of particles,  $f_\alpha^{eq}$  is the local equilibrium distribution function,  $e = \frac{\Delta x}{\Delta t}$ ,  $\Delta t$  is the time step,  $\Delta x$  is the lattice size,  $x$  is the space vector defined by the Cartesian coordinate system,  $F$  is the component of the force in  $x$  direction,  $\tau$  is the single relaxation time,  $N_\alpha$  is a constant, which

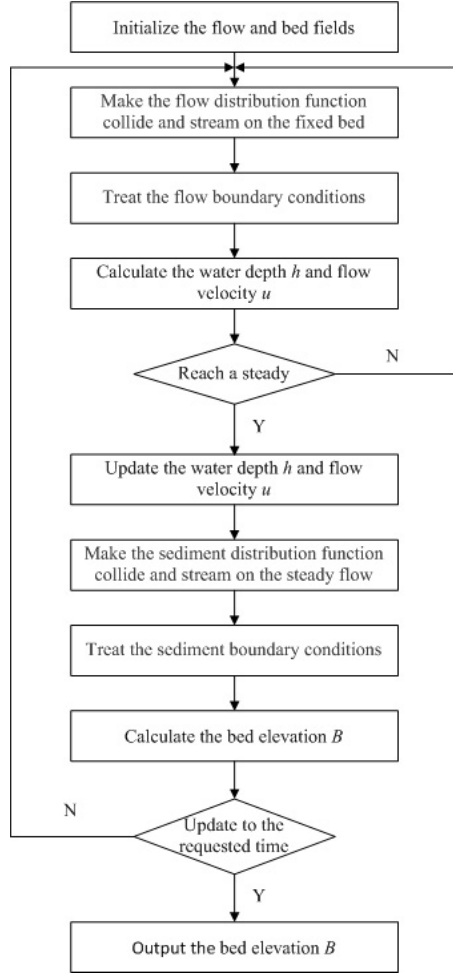


Fig. 1. Flow diagram of the algorithm

is equal to 2 for the D1Q3 lattice [Zhou, 2002]. The velocity vector of particles  $e_\alpha$  is given as follows:

$$e_\alpha = \begin{cases} 0, & \alpha = 0, \\ e, & \alpha = 1, \\ -e, & \alpha = 2, \end{cases} \quad (7)$$

Additionally, the macroscopic variables, the water depth  $h$  and the velocity  $u$ , are defined as

$$h = \sum_{\alpha} f_{\alpha}, \quad u = \frac{1}{h} \sum_{\alpha} e_{\alpha} f_{\alpha}. \quad (8)$$

6 *L. CAI, W.J. XU & X.Y. LUO*

The local equilibrium distribution function, determined by  $h$  and  $u$ , is defined as

$$f_{\alpha}^{eq} = \begin{cases} h - \frac{gh^2}{2e^2} - \frac{hu^2}{e^2}, & \alpha = 0, \\ \frac{gh^2}{4e^2} + \frac{hu}{2e} + \frac{hu^2}{2e^2}, & \alpha = 1, \\ \frac{gh^2}{4e^2} - \frac{hu}{2e} + \frac{hu^2}{2e^2}, & \alpha = 2, \end{cases} \quad (9)$$

whose calculating process is described in the literature [Liu *et al.*, 2015].

In our DDF-LBM, the D1Q3 model mentioned above is introduced to solve the shallow water equations for a fixed bed. Through the Chapman-Enskog expansion, the 1D shallow water equations can be recovered from the lattice Boltzmann equation (6). This allows us to determine the hydrological variables, water depth  $h$  and velocity  $u$ , from the D1Q3 lattice model.

#### 2.4. Lattice Boltzmann model for the Exner equation

Since the hydrological variables can be known from the proposed D1Q3 model, it's time to calculate the river-bed deformation by using the other lattice Boltzmann model. In order to solve the Exner equation, two lattice models with three and five particle velocities (D1Q3 and D1Q5), are used in this section.

##### 2.4.1. Lattice Boltzmann equation

We start with the following evolution equation:

$$g_{\alpha}(x + e_{\alpha}\Delta t, t + \Delta t) - g_{\alpha}(x, t) = -\frac{1}{\tau}(g_{\alpha} - g_{\alpha}^{eq}), \quad (10)$$

where  $\Delta t$ ,  $\Delta x$ , and  $\tau$  are defined as above,  $e_{\alpha}$  still stands for the velocity of particles, but will be three and five velocities. While,  $g_{\alpha}$  and  $g_{\alpha}^{eq}$  are the distribution function and the local equilibrium distribution function for the Exner equation, respectively. We assume the distribution function  $g_{\alpha}$  controls the local equilibrium distribution function  $g_{\alpha}^{eq}$ , and meets the condition

$$\sum_{\alpha} g_{\alpha}(x, t) = \sum_{\alpha} g_{\alpha}^{eq}(x, t). \quad (11)$$

Now we define the bed elevation  $B$  in the distribution function as

$$B(x, t) = \sum_{\alpha} g_{\alpha}(x, t), \quad (12)$$

which is the macroscopic variable to be determined.

Evidently, the choice of local equilibrium distribution function  $g_{\alpha}^{eq}$  is the key of the model. Only when an appropriate  $g_{\alpha}^{eq}$  is defined can we get the right riverbed solution from the lattice Boltzmann equation (10). In the LBM, the local equilibrium distribution function is determined by the method of undetermined coefficients [He *et al.*, 2008; Mohamad, 2011]. In general, the local equilibrium distribution function is expressed as a power series with some unknown constants, and then calculate the

unknowns according to the relevant conditions. The lattice model in this subsection is used to recover the Exner equation. Hence the following conditions should hold,

$$\sum_{\alpha} g_{\alpha}^{eq} = B, \quad (13)$$

$$\sum_{\alpha} e_{\alpha} g_{\alpha}^{eq} = \xi A u^3. \quad (14)$$

In these conditions, we choose  $e_{\alpha}$  from Eq. (7), the local equilibrium distribution function with three particle velocities is obtained:

$$g_{\alpha}^{eq} = \begin{cases} B - \frac{9}{5e^2} \xi^2 A^2 u^5, & \alpha = 0, \\ \frac{1}{2e^2} (\xi A u^3 e + \frac{9}{5} \xi^2 A^2 u^5), & \alpha = 1, \\ \frac{1}{2e^2} (-\xi A u^3 e + \frac{9}{5} \xi^2 A^2 u^5), & \alpha = 2. \end{cases} \quad (15)$$

Based on the five-velocity lattice,

$$e_{\alpha} = \begin{cases} 0, & \alpha = 0, \\ e \cos[(\alpha - 1)\pi], & \alpha = 1, 2, \\ 2e \cos[(\alpha - 1)\pi], & \alpha = 3, 4, \end{cases} \quad (16)$$

and  $g_{\alpha}^{eq}$  for the Exner equation is

$$g_{\alpha}^{eq} = \begin{cases} B - \frac{9}{4e^4} (\xi^2 A^2 u^5 e^2 - \xi^4 A^4 u^9), & \alpha = 0, \\ \frac{1}{6e^4} (4\xi A u^3 e^3 + \frac{36}{5} \xi^2 A^2 u^5 e^2 - 9\xi^4 A^4 u^9 - \frac{27}{7} \xi^3 A^3 u^7 e), & \alpha = 1, \\ \frac{1}{6e^4} (-4\xi A u^3 e^3 + \frac{36}{5} \xi^2 A^2 u^5 e^2 - 9\xi^4 A^4 u^9 + \frac{27}{7} \xi^3 A^3 u^7 e), & \alpha = 2, \\ \frac{1}{24e^4} (\frac{54}{7} \xi^3 A^3 u^7 e - 2\xi A u^3 e^3 + 9\xi^4 A^4 u^9 - \frac{9}{5} \xi^2 A^2 u^5 e^2), & \alpha = 3, \\ \frac{1}{24e^4} (-\frac{54}{7} \xi^3 A^3 u^7 e + 2\xi A u^3 e^3 + 9\xi^4 A^4 u^9 - \frac{9}{5} \xi^2 A^2 u^5 e^2), & \alpha = 4. \end{cases} \quad (17)$$

#### 2.4.2. Recovery of the Exner equation

Through the Chapman-Enskog expansion, the Exner equation (3) can be derived from the lattice Boltzmann equation (10), which is used to prove the bed elevation resulted from Eq. (12) is the correct solution for bed-load sediment transport. The derivation processes of D1Q3 and D1Q5 model are similar, so we choose the former to explain in the following.

We assume that the time step  $\Delta t$  is small and equal to the Knudsen number  $\varepsilon$  [Yan, 2000],

$$\Delta t = \varepsilon. \quad (18)$$

Substituting Eq. (18) into Eq. (10), we have

$$g_{\alpha}(x + e_{\alpha}\varepsilon, t + \varepsilon) - g_{\alpha}(x, t) = -\frac{1}{\tau}(g_{\alpha} - g_{\alpha}^{eq}). \quad (19)$$



8 *L. CAI, W.J. XU & X.Y. LUO*

Using the Taylor expansion to the left-hand side of the above equation in time and space at point  $(x, t)$  leads to

$$\varepsilon\left(\frac{\partial}{\partial t} + e_\alpha \frac{\partial}{\partial x}\right)g_\alpha + \frac{1}{2}\varepsilon^2\left(\frac{\partial}{\partial t} + e_\alpha \frac{\partial}{\partial x}\right)^2g_\alpha + O(\varepsilon^3) = -\frac{1}{\tau}(g_\alpha - g_\alpha^{eq}). \quad (20)$$

According to the Chapman-Enskog expansion [Chapman and Cowling, 1970],  $g_\alpha$  can be expanded around  $g_\alpha^{(0)}$ , having

$$g_\alpha = g_\alpha^{(0)} + \varepsilon g_\alpha^{(1)} + \varepsilon^2 g_\alpha^{(2)} + O(\varepsilon^3). \quad (21)$$

Thus, Eq. (20) to order  $\varepsilon^{(0)}$  is

$$g_\alpha = g_\alpha^{eq}, \quad (22)$$

to order  $\varepsilon$  is

$$\left(\frac{\partial}{\partial t} + e_\alpha \frac{\partial}{\partial x}\right)g_\alpha^{(0)} = -\frac{1}{\tau}g_\alpha^{(1)}, \quad (23)$$

to order  $\varepsilon^2$  is

$$\left(\frac{\partial}{\partial t} + e_\alpha \frac{\partial}{\partial x}\right)g_\alpha^{(1)} + \frac{1}{2}\left(\frac{\partial}{\partial t} + e_\alpha \frac{\partial}{\partial x}\right)^2g_\alpha^{(0)} = -\frac{1}{\tau}g_\alpha^{(2)}. \quad (24)$$

Substitution Eq. (23) into Eq. (24) gives

$$\left(1 - \frac{1}{2\tau}\right)\left(\frac{\partial}{\partial t} + e_\alpha \frac{\partial}{\partial x}\right)g_\alpha^{(1)} = \frac{1}{\tau}g_\alpha^{(2)}. \quad (25)$$

Taking  $\sum_\alpha$ (23) +  $\varepsilon$ (24) about  $\alpha$ , we have

$$\begin{aligned} \frac{\partial}{\partial t} \sum_\alpha g_\alpha^{(0)} + \frac{\partial}{\partial x} \sum_\alpha e_\alpha g_\alpha^{(0)} + \varepsilon\left(1 - \frac{1}{2\tau}\right)\frac{\partial}{\partial t} \sum_\alpha g_\alpha^{(1)} + \varepsilon\left(1 - \frac{1}{2\tau}\right)\frac{\partial}{\partial t} \sum_\alpha e_\alpha g_\alpha^{(1)} = \\ -\frac{1}{\tau} \sum_\alpha g_\alpha^{(1)} - \frac{\varepsilon}{\tau} \sum_\alpha g_\alpha^{(2)}. \end{aligned} \quad (26)$$

Due to the conservation condition Eq. (11), the following relations are obtained

$$\sum_\alpha g_\alpha^{(1)} = \sum_\alpha g_\alpha^{(2)} = 0, \quad \frac{\partial}{\partial t} \sum_\alpha g_\alpha^{(1)} = 0. \quad (27)$$

Now simplifying Eq. (26) with the relations (27), we have

$$\frac{\partial}{\partial t} \sum_\alpha g_\alpha^{(0)} + \frac{\partial}{\partial x} \sum_\alpha e_\alpha g_\alpha^{(0)} + \varepsilon\left(1 - \frac{1}{2\tau}\right)\frac{\partial}{\partial x} \sum_\alpha e_\alpha g_\alpha^{(1)} = 0. \quad (28)$$

Substituting Eq. (23) into the above equation leads to

$$\begin{aligned} \frac{\partial}{\partial t} \sum_\alpha g_\alpha^{(0)} + \frac{\partial}{\partial x} \sum_\alpha e_\alpha g_\alpha^{(0)} = \\ \varepsilon\left(\tau - \frac{1}{2}\right)\frac{\partial}{\partial x} \sum_\alpha e_\alpha e_\alpha \frac{\partial}{\partial x} g_\alpha^{(0)} + \varepsilon\left(\tau - \frac{1}{2}\right)\frac{\partial}{\partial x} \sum_\alpha e_\alpha \frac{\partial}{\partial t} g_\alpha^{(0)}. \end{aligned} \quad (29)$$

Because the value of  $\varepsilon$  is small and the riverbed is updated in a steady flow condition. After substituting Eq. (13) and Eq. (14) into (29) with the relation (22), the Exner equation can be obtained from the LBM dynamics

$$\frac{\partial B}{\partial t} + \frac{\partial \xi A u^3}{\partial x} = 0. \quad (30)$$

### 2.5. Boundary conditions

In this section, the boundary conditions of the DDF-LBMs will be discussed. The computation domain is  $[0, L]$ . Firstly, we consider the D1Q3 DDF-LBM, in which both the flow and sediment distribution function are based on three particle velocities. Its clear that four boundary conditions should be handling. At  $x_0$ , the left-hand boundary condition, the value of  $f_2, g_2$  can be obtained from the streaming process, while the  $f_1$  and  $g_1$  are unknown. The right margin,  $x_N$ , is just the opposite:  $f_2$  and  $g_2$  are unknown.

In general, many different boundary conditions can be used. But since the velocity and the depth of flow and the bed elevation are known in this model; we use the bounce-back scheme in this paper [He *et al.*, 2008]. The unknown distribution functions are decided as

$$f_1|_{x_0} = f_2|_{x_0}, \quad g_1|_{x_0} = g_2|_{x_0}, \quad (31)$$

and

$$f_2|_{x_N} = f_1|_{x_N}, \quad g_2|_{x_N} = g_1|_{x_N}, \quad (32)$$

where  $N$  is the total number of the discrete grids.

Like the previous model, we also use the bounce-back scheme in the D1Q5 DDF-LBM, in which the flow distribution function is with three particle velocities, while the sediment distribution function is with five. In this DDF-LBM, eight boundary conditions should be handling. At  $x_0$ , the left-hand boundary condition, the value of  $f_1, g_1$  and  $g_3$  are unknown. The right margin,  $x_N$ , is the opposite:  $f_2, g_2$  and  $g_4$  are unknown. In addition, different from the D1Q3 DDF-LBM, the values of  $g_3$  at  $x_1$  and  $g_4$  at  $x_{N-1}$  are also required. The unknown distribution functions are decided as follows:

At  $x_0$ :

$$f_1|_{x_0} = f_2|_{x_0}, \quad g_1|_{x_0} = g_2|_{x_0}, \quad g_3|_{x_0} = g_4|_{x_0}. \quad (33)$$

At  $x_1$ :

$$g_3|_{x_1} = g_4|_{x_1}. \quad (34)$$

At  $x_{N-1}$ :

$$g_4|_{x_{N-1}} = g_3|_{x_{N-1}}. \quad (35)$$

10 *L. CAI, W.J. XU & X.Y. LUO*

At  $x_N$ :

$$f_2|_{x_N} = f_1|_{x_N}, g_2|_{x_N} = g_1|_{x_N}, g_4|_{x_N} = g_3|_{x_N}. \quad (36)$$

We note that the bounce-back scheme is not the only method, other options may also be chosen as appropriate.

### 3. Numerical tests

To examine the efficacy of two DDF-LBMs, two tests, wave propagation test problem and channel test problem, are studied in this section. For the first one, the riverbed is fixed. It is used to illustrate the accuracy of the D1Q3 lattice model [Zhou, 2002] for the shallow water equations. The last one is for the riverbed deformation. In realization, there are a large number of discrete points. In order to keep the image clarity, only a part of the points are shown in our figures.

#### 3.1. Wave propagation problem

The wave propagation problem with a pulse present in the riverbed can be described by the shallow water equations. The test problem is taken from LeVeque [Le Veque, 1998] and Feng [Feng *et al.*, 2006], consisting a 1D channel of length 1. The initial conditions are

$$u(x, 0) = 0, h(x, 0) = \begin{cases} 1 + \omega - B(x, 0), & \text{if } 0.1 \leq x \leq 0.2, \\ 0.5, & \text{otherwise,} \end{cases} \quad (37)$$

and the bottom topography takes the form

$$B(x, 0) = \begin{cases} \frac{1}{4}(\cos(\frac{\pi(x-0.5)}{0.1}) + 1), & \text{if } |x - 0.5| < 0.1, \\ 0, & \text{otherwise.} \end{cases} \quad (38)$$

Following Le Veque and Feng, the value of  $\omega$  is taken as 0.2, and the gravitational constant  $g$  is 10.

For this problem, the grid with 1000 cells is used, together with the relaxation time  $\tau = 0.6$ . The boundary conditions on  $x_0$  and  $x_N$  are shown in (31) and (32) respectively. We obtain the numerical results in Figs. 2, 3 and 4. Fig. 2 shows the bottom topography and the water surface at time  $t = 0.7$ , while the water depth  $h$  and velocity  $u$  over the hump are shown in Figs. 3 and 4. In order to examine its accuracy, we use a reference solution (RS) as the comparison one. The RS is based on the CWENO-type central-upwind finite difference schemes and has fifth-order accuracy in smooth regions [Feng *et al.*, 2006].

From Figs. 2 to 4, excellent agreements are obtained in the water surface  $h + B$  and depth  $h$ , while the water velocity  $u$  looks a little different from the RS. This is presumably because the RS we used here is based on the fifth-order schemes. This relatively low and cannot meet such a high accuracy. By comparing the numerical solution (NS) with RS, we can see that the accurate results have been produced

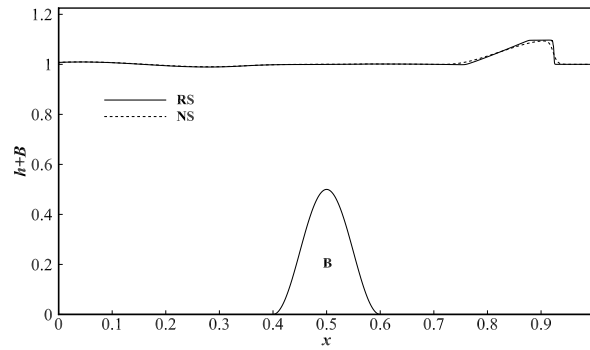


Fig. 2. The water surface at time  $t = 0.7$  and bottom topography

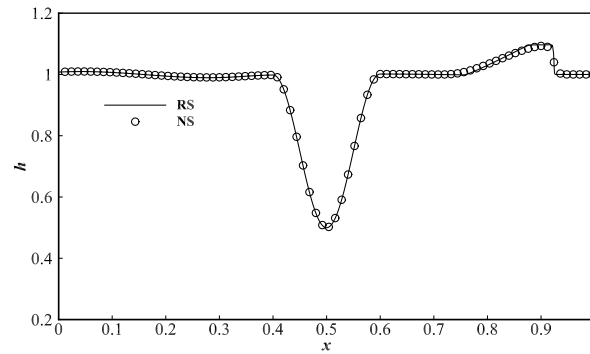


Fig. 3. The water depth at time  $t = 0.7$

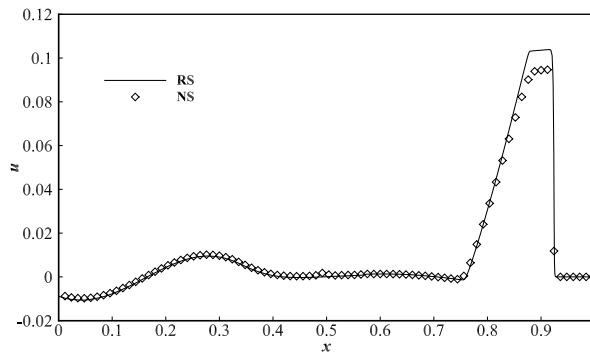


Fig. 4. The water velocity at time  $t = 0.7$

from the D1Q3 flow lattice model at time  $t = 0.7$ . Therefore, the D1Q3 flow lattice model for the shallow water equations is accurate, and can be used to develop the DDF-LBMs.

### 3.2. The channel test problem

The previous section discussed the correctness of the flow lattice model. Now, We will check the efficiency of the D1Q3 and D1Q5 DDF-LBMs for the bed-load sediment transport. The test case is taken from Hudson [Hudson, 2001]. It consists of a channel of length 1000 with the following dummy initial conditions

$$u^*(x, 0) = \frac{Q}{h^*(x, 0)}, \quad h^*(x, 0) = D - B(x, 0), \quad (39)$$

where the discharge  $Q$  and the water surface  $D$  are constant whose value is 10 in this paper. And the bottom topography is

$$B(x, 0) = \begin{cases} \sin^2\left(\frac{\pi(x-300)}{200}\right), & \text{if } 300 \leq x \leq 500, \\ 0, & \text{otherwise.} \end{cases} \quad (40)$$

As we know, the shallow water equations and Exner equation should be solved in turn to obtain a realistic result of the river-bed deformation. When we calculate the water depth  $h$  and velocity  $u$ , the river-bed is fixed. When the river-bed  $B$  is solved, the hydrological variables are fixed. We always fix one and solve the other one. Thus, the consistency of the water flow and bed is important in the initial conditions and will impact the stability of the model. However, the initial flow condition in this test is a dummy one. So, we fix the riverbed and iterate the water flow in the flow LBM model to an equilibrium state. This equilibrium state means the absolute change in velocity between current and last iterations is less than  $1.0 \times 10^{-6}$ . The results are illustrated in Figs. 5 and 6.

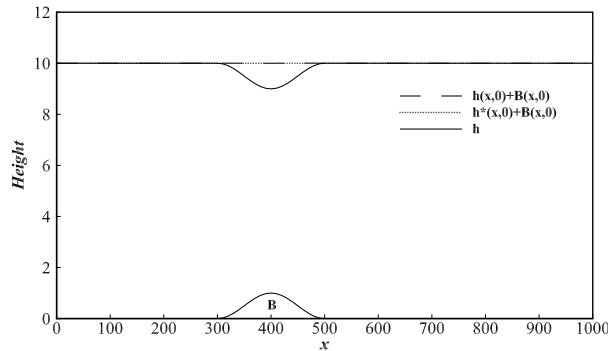
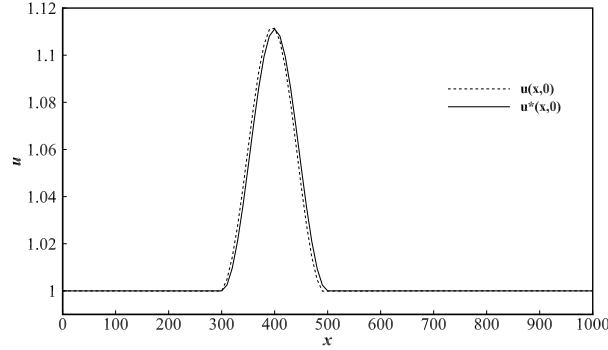


Fig. 5. The water surface and depth of real initial conditions

From Figs. 5 and 6, we can see that the real initial conditions are roughly coincidence to the dummy one. This means the dummy conditions of the water flow are consistent with the bed.

The consistency between the water flow and the bed has been verified. Next we should calculate the river-bed. Before this, an approximate solution (AS) will be

Fig. 6. The water velocity  $u$  of real initial conditions

given for this problem. In the case, the total height of the river and the discharge throughout the whole domain are constant, which makes it has an AS [Hudson, 2001]. For the sediment transport flux  $q(u) = Au^3$ , the AS of river-bed  $B(x, t)$  is

$$B(x, t) = \begin{cases} \sin^2\left(\frac{\pi(x-300)}{200}\right), & \text{if } 300 \leq x \leq 500, \\ 0, & \text{otherwise,} \end{cases} \quad (41)$$

where the value of  $x$  is determined by  $x_0$  and  $t$ . The formulate of  $x$  is

$$x = x_0 + 3A\xi Q|Q|^2t \begin{cases} (10 - \sin^2\left(\frac{\pi(x_0-300)}{200}\right))^{-4}, & \text{if } 300 \leq x_0 \leq 500, \\ 10^{-4}, & \text{otherwise.} \end{cases} \quad (42)$$

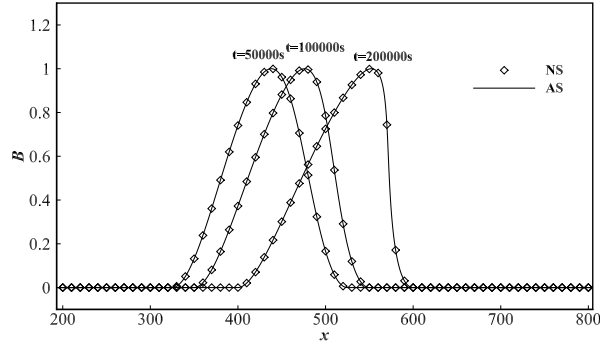
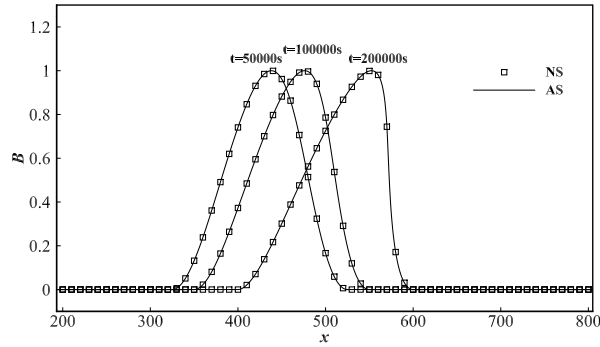
With this AS, we will verify further the effectiveness of our D1Q3 and D1Q5 DDF-LBMs.

In this problem, we use the grid with 1000 cells, and set the parameters  $A = 0.001$ ,  $\Delta t = 0.1$ ,  $\tau = 1$ . The boundary conditions on  $x_0$  and  $x_N$  are offered from (31) to (36). The numerical results of double-distribution-function LBM models at  $t = 50000s$ ,  $t = 100000s$  and  $200000s$  are obtained. The AS and NS of the D1Q3 DDF-LBM are shown in Fig. 7, while Fig. 8 shows the results of the D1Q5 DDF-LBM.

From Figs. 7 and 8, it can be seen that as time goes on, the river-bed is changing gradually. By comparing the NS with AS, we can conclude that the excellent agreements have been obtained between the NS and AS. That means the D1Q3 and D1Q5 DDF-LBMs proposed in the section 2 are accurate. Therefore, both the DDF-LBMs in our research can be used to simulate the 1D bed-load sediment transport correctly, and have a definite application value.

Of course, the calculation of bed elevation is the key of the sediment transport. In order to further compare the accuracy of the D1Q3 and D1Q5 DDF-LBMs, the error based on the 2-norm is defined for the bed elevation, which is

$$Er = \left[ \sum_{i=1}^N (B_i^{NS} - B_i^{NA})^2 \right]^{\frac{1}{2}}, \quad (43)$$

Fig. 7. The bed elevation  $B$  in the D1Q3 DDF-LBMFig. 8. The bed elevation  $B$  in the D1Q5 DDF-LBM

where  $N$  is the total number of the discrete grids,  $B_i^{NS}$  is the NS of the river-bed in the node  $i$ ,  $B_i^{AS}$  is the AS of the river-bed in the node  $i$ . The errors of two DDF-LBMs are presented in Table 1.

Table 1. The 2-norm errors of D1Q3, D1Q5 DDF-LBMs and FDM [Hudson, 2003].

Times	D1Q3	D1Q5	FDM
50000s	0.0139	0.0073	0.0158
100000s	0.0355	0.0082	0.0389
200000s	0.2195	0.0225	0.2013

As we can see from the Table 1, both errors of the DDF-LBMs are small. The error of the D1Q3 DDF-LBM and the FDM are almost the same. But the error of the D1Q5 DDF-LBM is smaller than errors of D1Q3 DDF-LBM and FDM. Based on analysing characteristics of the 2-norm errors for the D1Q3 and D1Q5 DDF-LBMs, we can find that the DDF-LBM with five-velocity lattice is more accurate.

It offers better accuracy than the D1Q3, although with an increased cost.

#### 4. Conclusions

Two DDF-LBMs for 1D sediment transport based on the quasi-steady approach are presented in this paper. Both of the D1Q3 and D1Q5 DDF-LBMs can be used to obtain the numerical approximation of the equations governing sediment transport. The basic features of them are that they can be formulated on a natural extension of the local equilibrium distribution functions and can offer a simple procedure, while keeping the better efficiency. This makes the DDF-LBM a good method for the large-scale practical sediment transport problems. Two numerical tests are used to demonstrate the simplicity, accuracy and efficiency of our DDF-LBMs.

#### Acknowledgements

This work was supported by the National Natural Science Foundation of China (11471261, 11101333, 11302172).

#### References

- Aminfar, H., Razmara, N., Mohammadpourfard, M. [2015] “Molecular dynamics study of aggregation in nanofluid flow: effects of liquid-nanoparticle interaction strength and particles volume fraction,” *International Journal of Applied Mechanics* **7(01)**, 1550010.
- Bég, O. A., Bég, T. A., Rashidi, M. M., Asadi, M. [2013] “DTM-Padé semi-numerical simulation of nanofluid transport in porous media,” *International Journal of Applied Mathematics and Mechanics* **9**, 10–32.
- Cunge, J. A., Holly, F. M. and Verwey, A. [1980] *Practical aspects of computational river hydraulics* (Pitman Advanced Pub. Program, Pitman).
- Chen, S. Y. and Doolen, G. D. [2003] “Lattice Boltzmann method for fluid flows,” *Annual Review of Fluid Mechanics* **30**, 329–364.
- Chapman, S. and Cowling, T. G. [1970] *The Mathematical Theory of Non-uniform Gas* (Cambridge University Press, Cambridge).
- De Vriend, H. J., Zyserman, J., Nicholson, J., Roelvink, J. A., Pechon, P., and Southgate, H. N. [1993] “Medium-term 2DH coastal area modelling,” *Coast. Eng.* **21**, 193–224.
- Feng, J. H., Cai, L., Xie, W. X. [2006] “CWENO-type central-upwind schemes for multidimensional Saint-Venant system of shallow water equations,” *Applied Numerical Mathematics* **56**, 1001–1017.
- Grass, A. J. [1981] “Sediment transport by waves and currents,” *SERC London, Cent. Mar. Technol.* **FL29**.
- Hudson, J. and Sweby, P. K. [2003] “Formulations for Numerically Approximat-



- ing Hyperbolic Systems Governing Sediment Transport,” *Journal of Scientific Computing* **19**, 225–252.
- Hudson, J. [2001] “Numerical Techniques for Morphodynamic Modelling,” Ph.D. thesis, Mathematics Dept., University of Reading, Reading.
- He, Y. L., Wang, Y. and Li, Q. [2008] *Lattice Boltzmann Method: Theory and Applications (in Chinese)* (Beijing Science Press, Beijing).
- Liu, H., Ding, Y., Li, M., Lin, P., Yu, M. H. and Shu, A. P. [2014] “A hybrid lattice Boltzmann method finite difference method model for sediment transport and riverbed deformation,” *River Research and Applications* **31**, 447–456.
- Liu, H., Wang, H., Liu, S., Hu, C. W., Ding, Y., Zhang, J. [2015] “Lattice Boltzmann method for the Saint-Venant equations,” *Journal of Hydrology* **524**, 411–416.
- Le Veque R. J. [1998] “Balancing Source Terms and Flux Gradients in High-Resolution Godunov Methods: The Quasi-Steady Wave-Propagation Algorithm,” *Journal of Computational Physics* **146**, 346–365.
- Moeendarbary, E., Ng, T. Y., Zangeneh, M. [2009] “Dissipative particle dynamics: introduction, methodology and complex fluid applications a review,” *International Journal of Applied Mechanics* **1(4)**, 737–763.
- Mohamad, A. A. [2011] *Lattice Boltzmann Method: Fundamentals and engineering applications with computer codes* (Springer, London).
- Salmon, R. [1999] “The lattice Boltzmann method as a basis for ocean circulation modeling,” *Journal of Marine Research* **57**, 503–535.
- Soulsby, R. L. [1997] “Dynamics of Marine Sands: a Manual for Practical Applications,” *HR Wallingford* **SR 466**.
- Thang, P. V., Chopard, B. and Lefèvre, L. [1997] “Study of the 1D lattice Boltzmann shallow water equation and its coupling to build a canal network,” *Journal of Computational Physics* **229**, 7373–7400.
- Yan, G. W. [2000] “A lattice Boltzmann equation for waves,” *J. Comput. Phys.* **161**, 61–69.
- Zhou, J. G. [2002] “A lattice Boltzmann model for the shallow water equations,” *Comput. Methods Appl. Mech. Eng.* **191**, 3527–3539.
- Zhou, J. G. [2009] “A lattice Boltzmann method for solute transport,” *Int. J. Numer. Meth.* **61**, 848–863.